Supplement of Nat. Hazards Earth Syst. Sci., 24, 3445–3460, 2024
https://doi.org/10.5194/nhess-24-3445-2024-supplement

Natural Hazards and Earth System Sciences
Open Access
EGU

Supplement of

Insurance loss model vs. meteorological loss index – how comparable are their loss estimates for European windstorms?

Julia Moemken et al.

Correspondence to: Julia Moemken (julia.moemken@kit.edu)

S1. Documentation of European Windstorm Model of Aon Impact Forecasting

Impact Forecasting European Windstorm Model - Overview

22 July 2024

Table of Contents

1 Introduction

This document provides an overview of the Impact Forecasting (IF) European Windstorm (EUWS) model. It includes a summary of the most important model characteristics and is an abridged version of the full model documentation. The full documentation is proprietary and typically available only to model licensees, while this overview is intended for wider circulation. This document is not intended to support users of the EUWS model. Most of the practical information about model files, sensitivity and stability testing, vulnerability modifiers and model validation has not been included. This overview gives a description of the components of a catastrophe model, aimed at readers who are not working in this industry, followed by some description of each of those components in relation to the IF EUWS model.

The IF EUWS model was first released in 2014, updated in 2016, 2022, and most recently in 2023. Version 1.6, released in March 2023, covered 22 European countries as illustrated in Figure 1.

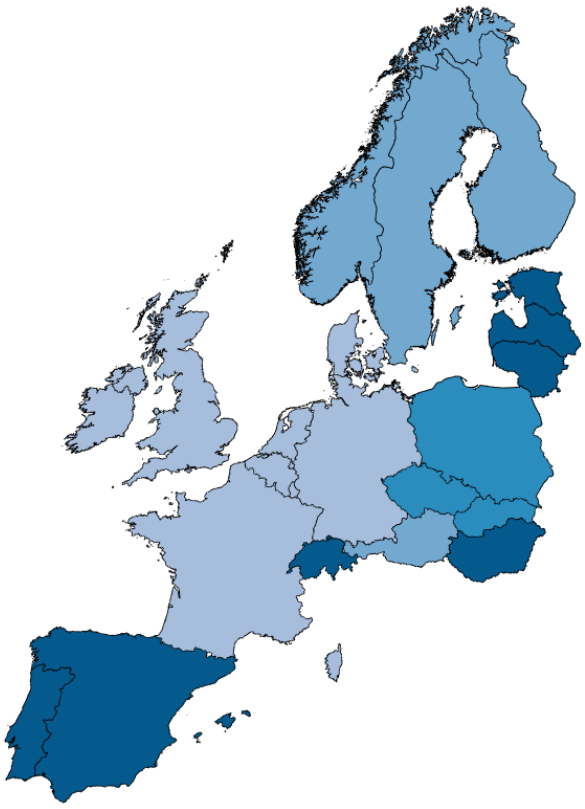

Figure 1 - Countries covered by the IF EUWS model. The shades of blue from light to dark correspond to the four stages of releases as described above.

2 Components of a Catastrophe Model

The catastrophe model estimates monetary damage caused by a certain peril. The key components (Figure 2) of a catastrophe model are:

1 Exposure

2 Hazard

3 Vulnerability

4 Loss

From the perspective of an end user, the first stage is the preparation of the exposure data, which describes the risks that are being modelled, and is typically the portfolio of a (re)insurance company. This input data must describe each risk individually (though a risk may contain many items aggregated into one value), giving as a minimum some characterization such as residential or motor, the location and total insured value (TIV), along with any additional information such as the size or type of building, that will allow the model to predict likely damages to each risk more accurately. The model will then geocode each risk, assigning it to a location in the model (1. Exposure). The model will then run through a set of events, which is the hazard component of the model, corresponding to the modelled peril, e.g. windstorm, flood or earthquake. For each event, there will be a hazard value such as gust speed, flood depth or ground shaking at the location of each risk (2. Hazard). The likely loss is estimated using the vulnerability function, which predicts damage based on the hazard intensity and given vulnerability function for each individual risk (3. Vulnerability). The losses are then aggregated, and financial conditions are applied before the results are output to the user for risk evaluation and financial modelling (4. Loss).

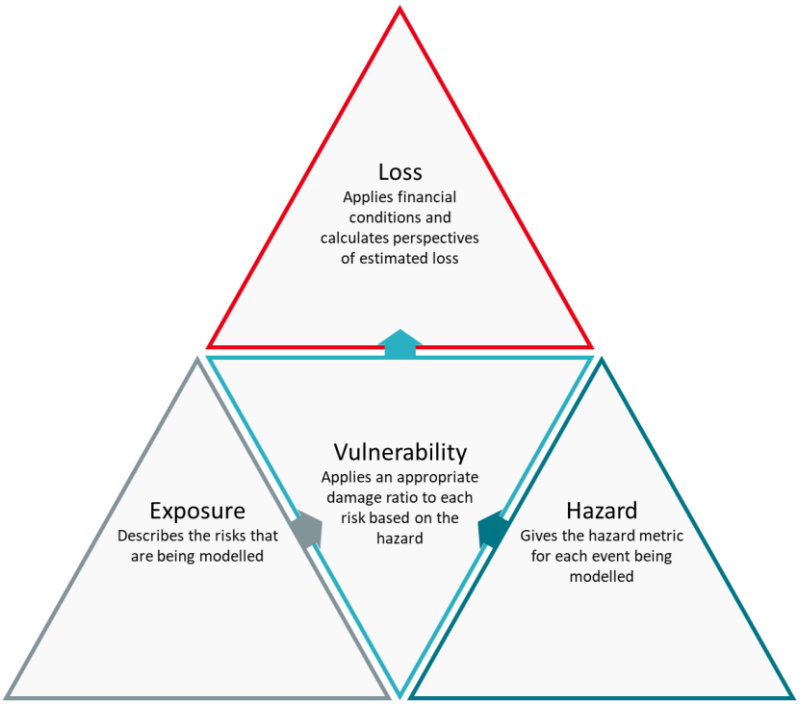

Figure 2 - Components of a catastrophe model.

3 Exposure Component and Geocoding

To match input locations in the model to hazard values, some geocoding is required. Some catastrophe models can be run at grid level, matching locations to hazard grid points using latitude and longitude. Most commonly risks are input using administrative units. The administrative units used in this model are postcode, CRESTA (www.cresta.org) and municipality. Exposure data is typically provided by (re)insurance companies and is formatted for input into catastrophe modelling platforms by analysts. In order to estimate a loss, the exposure data must contain:

1. Location: The postcode, CRESTA or Municipality in which the risk is located.
2. Risk characterization: The model must categorize each risk as either residential, commercial, industrial, agricultural, motor or forestry. Additional information in the exposure file may be given to assign the risk various modifiers as described below.
3. Total Insured Value (TIV): The model must have a TIV for each risk. Other financial conditions such as deductibles or reinsurance recoveries may also be present.

Each line in a portfolio could contain a single risk, such as one building, or could contain many risks aggregated to administrative level.

To estimate losses on a market level, an estimate of the TIV of all companies in a territory is required. One source of this information is PERILS (www.perils.org) who aggregate and anonymize exposure data in several European countries and provide CRESTA level aggregated total exposure estimates. Figure 3 shows the TIV per CRESTA for residential building in Germany.

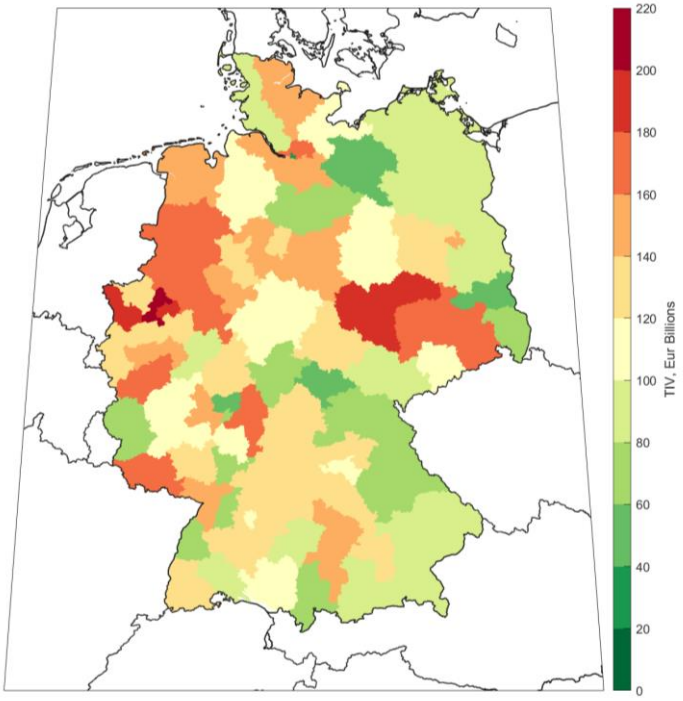

Figure 3 - Residential building TIV at CRESTA level in Germany, source: PERILS.

The IF EUWS model covers property, forestry and motor. Property is divided into four occupancies: residential, commercial, industrial, and agricultural. For each occupancy, there are optional modifiers for building size, roof type and construction material. The TIV for each property risk is divided into buildings, contents and time elements (also referred to as business interruption). At least one value must be given for each risk in a portfolio.

For forestry, the total forested area is used as an input. For motor, only the vehicle value is input as a building value.

4 Hazard Component

The hazard component of the model describes the peril, and in this case, it consists of footprints for windstorm events. There are both historical footprints for past storms and a stochastic catalogue of simulated, climate model generated storms. Users must select whether to run the historic or stochastic event set. The footprints in each set are formatted in the same way.

4.1 Historic Event Set

The model contains a set of 26 historical events. These are primarily a selection of the largest windstorms to affect Europe over the last 25 years, and some events with less impact on the continental level but significant impact on specific countries. The purpose of the historic event set is to be able to model the impact of historic events if they were to happen again with current exposure. This also enables companies to gain confidence in the model by comparing their experienced loss to the modelled loss.

For historic modelling, footprints are built directly from weather station data obtained via NOAA (https://www.ncei.noaa.gov). Inverse distance weighting is used to map station values to the model grid. Gusts are considered in terms of their relation to the climatology at each point rather than absolute values.

The storms included are: Daria (1990), Anatol (1999), Lothar (1999), Martin (1999), Erwin (2005), Kyrill (2007), Emma (2008), Klaus (2009), Xynthia (2010), Tappani (2011), Christian (2013), Xaver (2013), Dirk (2013), Tini (2014), Elon/Felix (2015), Mike/Niklas (2015), Thomas (2017), Zeus (2017), Xavier (2017), Herwart (2017), Eleanor (2018), Friederike (2018), Fabienne (2018), Isaias (2019), and Sabine (2020).

4.2 Stochastic Catalogue and Calibration

The stochastic storm catalogue of the model consists of 12044 simulated storms. These have been extracted from over 4000 years of ECHAM5 Global Circulation Model (GCM) simulations through a collaboration with academic partners at University of Cologne / Karlsruhe Institute of Technology (KIT). These synthetic storms are calibrated against a set of 124 historic storms taken from NCEP reanalysis data. Severe storms were identified within the NCEP reanalysis dataset (Kalnay et al., 1996) using a Loss Index (LI) described by Pinto et al (2012). The method is based on the original approach by Klawa and Ulbrich (2003) and is intended to identify storms that may cause a market impact (loss); thus, it focusses on the exceedance of the local 98th wind percentile. This is an advantage against an absolute wind or gust speed selection, which is liable to identify events with high values over sea or mountain grid points. The resolution of the reanalysis data was 2.5°x2.5°. The LI-method (Pinto et al., 2012) is applied to GCM output. The top 12044 storms from 4731 years of simulations were selected for use, corresponding to 2.55 storms per model year on average. More information about the generation of this dataset is given by Karremann et al. (2014). The resolution of the pre-downscaled stochastic storms is 1.875°x1.875°, approximately 200 x 200 km at mid-latitudes. The 124 historical events are used as a calibration event set. The goal of calibration is to correct biases in both gust intensity and occurrence frequencies of storms from the GCM. The GCM climatology is retained to preserve the temporal and seasonal clustering of the storms, as this is argued to be one of the key advantages of using the GCM.

The calibration process followed seven steps as follows:

1 Low resolution calibration.

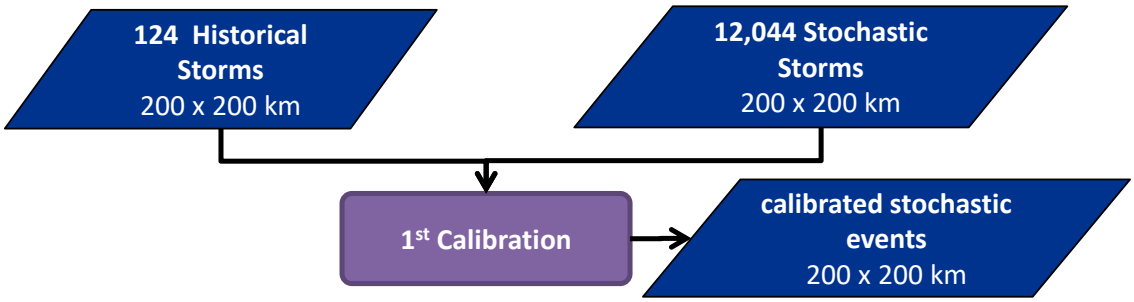

Figure 4 - Calibrating the GCM storm wind speed distributions against 50 years of historical reanalysis storms.

The 124 reanalysis storms are used to calibrate the wind speeds in the stochastic catalogue at course resolution. The aim of this stage is to address anomalies in the stochastic event set arising from biases in the GCM, e.g. too many zonal tracks. The wind speed distributions are adjusted using quantile-to-quantile matching per Weather Type, following the classification of Leckebusch et al. (2008).

2 Dynamical downscaling.

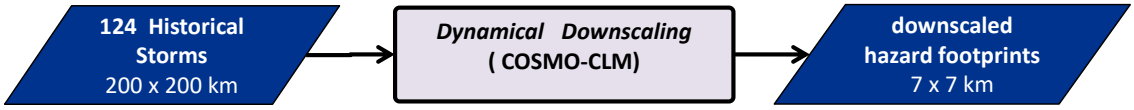

Figure 5 - Dynamical downscaling of the historic storms.

Each of the 124 storms were dynamically downscaled with the regional model COSMO-CLM (CCLM; Rockel et al., 2008) to 0.06125° resolution, approximately 7 km (see Born et al., 2012). For most events, a time window of 4 days is simulated to give sufficient lead time before the event peak. The COSMO-CLM model is forced (initial and boundary conditions) using ERA-40 and ERA-interim reanalysis data (Uppala et al., 2005; Dee et al., 2011). The resulting downscaled gust simulations were at two spatial resolutions: a 0.165° (~18km) domain and a nested 0.06125° (~7km) domain.

3 Statistical downscaling training.

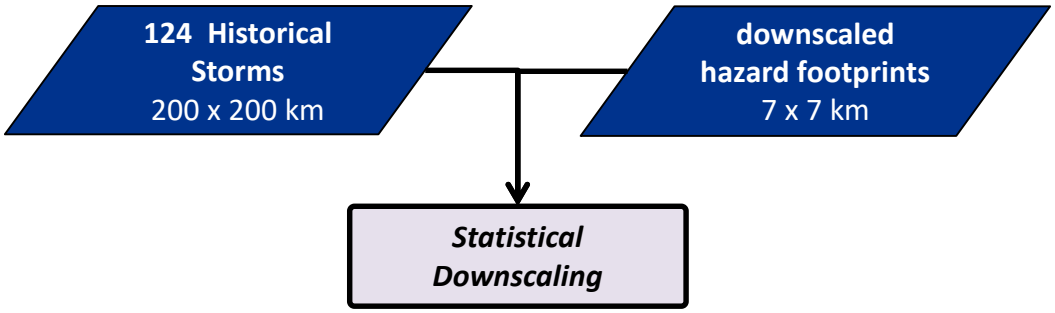

Figure 6 - Training of the statistical downscaling tool.

The 124 downscaled storms were used to train a statistical downscaling tool which could be applied to the stochastic event set (Haas and Pinto, 2012; Haas et al., 2014), A fully dynamically downscaling of the stochastic event set is not feasible due to its prohibitive computation costs. A multi-linear regression model was trained by comparing the NCEP wind

footprints to the CCLM gust footprints, in order to downscale them from the global scale to the same 7km resolution. A detailed account of this process is given by Haas and Pinto (2012) and Haas et al (2014). Figure 7 gives an illustration of the downscaling process for storm Xynthia.

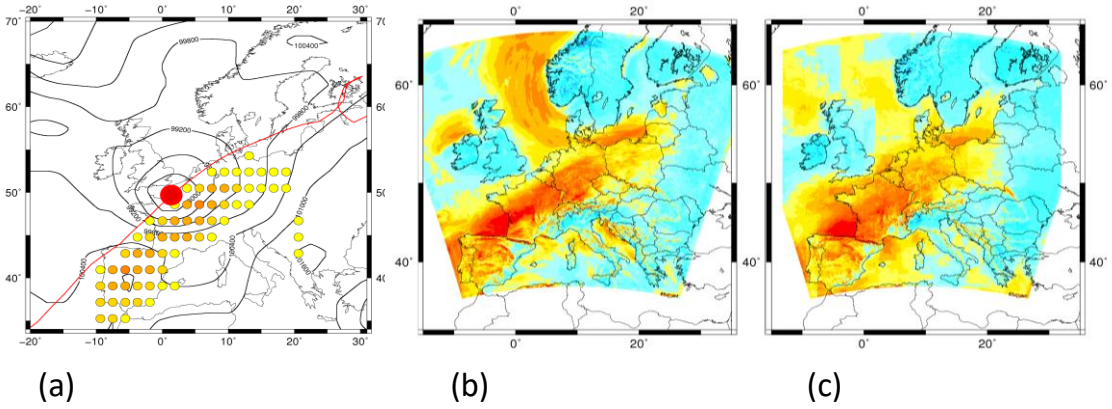

Figure 7 - Illustration of the application of the dynamical and statistical downscaling tools for storm Xynthia (2010); a) NCEP wind values at low resolution, b) RCM simulated dynamically downscaled gust footprint, c) gust footprint obtained from the statistical downscaling tool. (from Haas and Pinto, 2012, GRL)

4 Stochastic statistical downscaling.

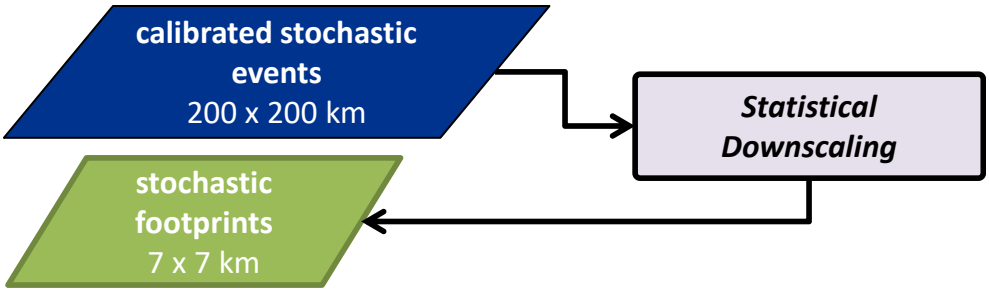

Figure 8 - Application of the statistical downscaling tool to the stochastic storms.

The low-resolution stochastic footprints - following calibration in step 1 - are downscaled to 0.0625° using the statistical downscaling tool developed in step 3. The low-resolution gridded gusts are input values and the output is gridded gusts on higher resolutions for each event.

5 High resolution calibration.

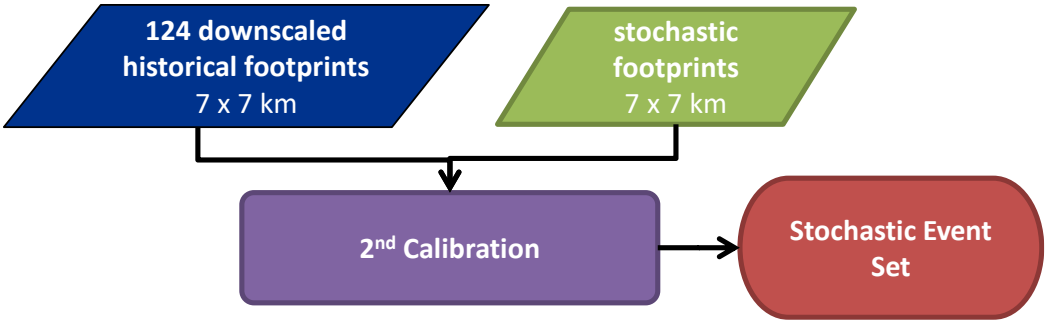

Figure 9 - Calibration of the high-resolution stochastic storms against high resolution reanalysis storms.

The downscaled stochastic gust footprints are now calibrated against the 124 historic footprints. The aim of this stage is to ensure the stochastic event set captures higher resolution features of gust footprints and to remove any unwanted artefacts or biases arising from the downscaling tool.

This calibration process is itself broken into two steps. The first focuses on the lower and middle parts of the gust distribution. At each grid point a quantile-to-quantile fitting is applied between the 10th and 98th gust percentiles. In most cases this is not affecting the gust speeds at which most loss is caused. The second step focuses on the tail of the gust distribution, above the 98th percentile, generally gusts with values above 30ms^{-1}. These values cannot be calibrated on a point-by-point basis because this would cause the stochastic gusts to be overly influenced by the impact of specific historical storms which dominate the tails of the gust distribution. The aim is instead to preserve the spatial patterns of the stochastic storms. The calibration is therefore done using four regions classified by height in meters above sea level (MASL); coastal (<15 MASL), lowland (15-100 MASL), midland (1-330 MASL), continental (>330 MASL). Gusts above the 99.5th percentile are not included. Regression functions are then built between the ranked stochastic and ranked historic gusts between the 98th and 99.5th percentiles within each domain and applied to the stochastic event set up to the 100th percentile.

The storms in the stochastic event are assigned to the simulated GCM years. The shape, track and regions affected by any storm is closely linked to the weather type at time of occurrence. As the distribution of WTs within the stochastic event set should closely resemble that of the historic event set, a correction is applied to counter any biases within the stochastic set towards or against specific weather types. This is done by adjusting the frequency of the stochastic years.

A known weakness of the COSMO-CLM model is that gusts at high altitudes may be overestimated in some cases (Born et al., 2012). In loss modelling, this issue is exacerbated by most risks in high altitude grid points being likely to exist below the average altitude of that model grid point, for example in valleys within mountainous areas. Based on an assumption that this is the case, gusts in grid points with altitudes above 850 MASL are reduced, assuming a logarithmic wind and gust profile, to the estimated wind gust at 850 MASL. The equation used is:

$$U_2 = U_1 \frac{ln\left(\frac{h_2}{z_0}\right)}{ln\left(\frac{h_1}{z_0}\right)}$$

Where U_2 and U_1 are the gust speeds at heights h_2 and h_1 respectively and z_0 is the roughness length. A constant z_0 of 0.75m is used.

Following this set of adjustments, a number of localized calibrations are made to remove specific artefacts which may arise either from the GCM or the COSMO-CLM model. These may be poorly resolved localized topographical features or 'streaks' of gusts persisting into Eastern Europe due to inaccurate resolving of blocking or storm dissipation. These adjustments are based on the comparison of the historic event set to weather station data and appropriate adjustment before applying adjustments to the stochastic model. Figure 10 shows the final stochastic event set gusts at various return periods.

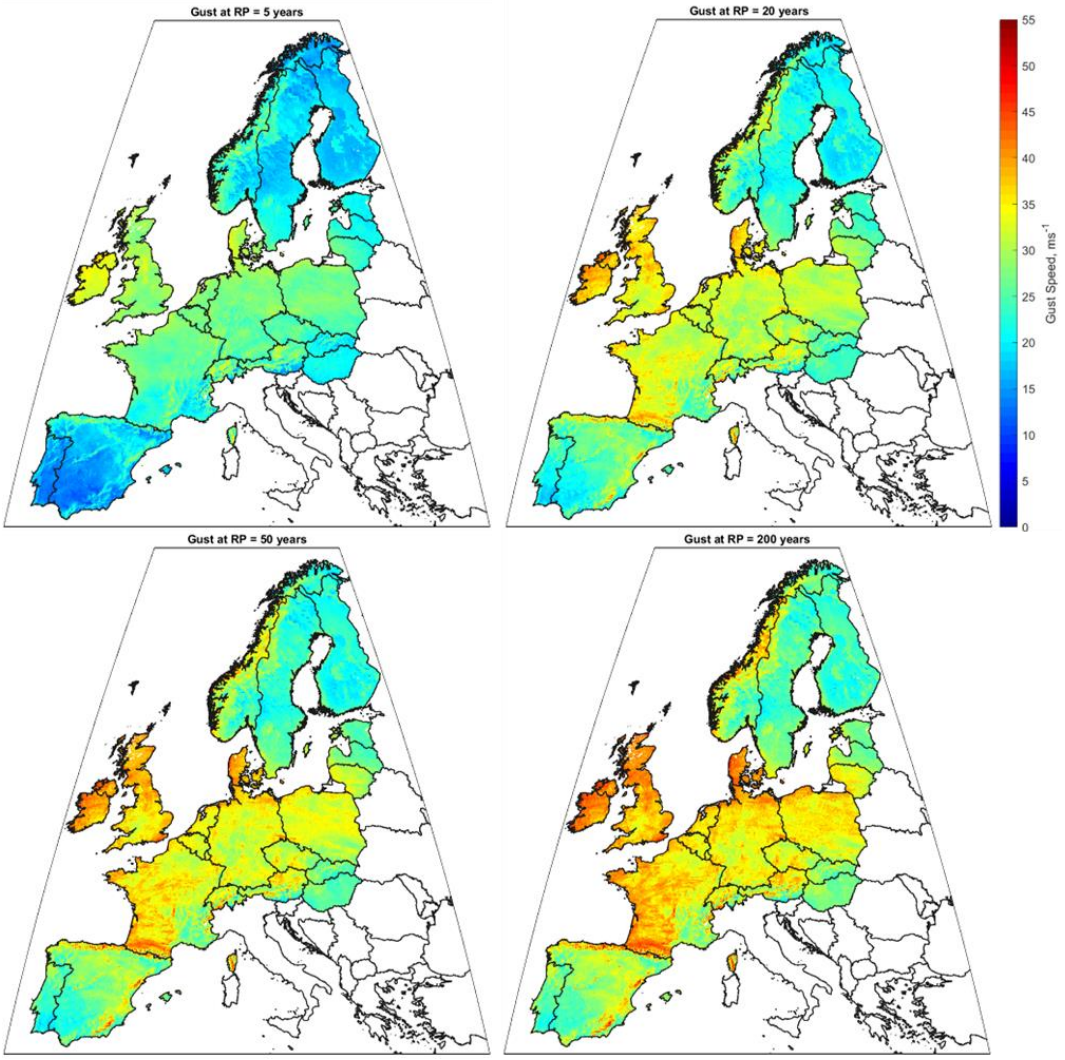

Figure 10 - Stochastic gusts at 5, 20, 50 and 200 years Return Periods.

The resulting hazard metric for the model is maximum wind gust. The background grid from which footprints are built is 7x7 km. Each point in this grid has a maximum gust value for that storm. The gust values are then mapped from this grid to administrative unit polygons using population weighting of the grid points. For forestry inverse population weighting is used. A distribution of gust values is given within each administrative unit as illustrated in Table 1, which shows the distribution of gust values in CRESTA 01 in Germany for an example event. The CRESTA is identified by its unique model ID and the gust values are listed with the associated probabilities. The probability values must sum to 1.

Event_ID	Location_ID	Gust	Prob
18	140276	30	0.2
18	140276	31	0.5
18	140276	32	0.3

Table 1 – Example model hazard showing the distribution of wind gust values in a CRESTA.

Figure 11 illustrated the maximum gust speed that covers at least 10% of each CRESTA in Germany.

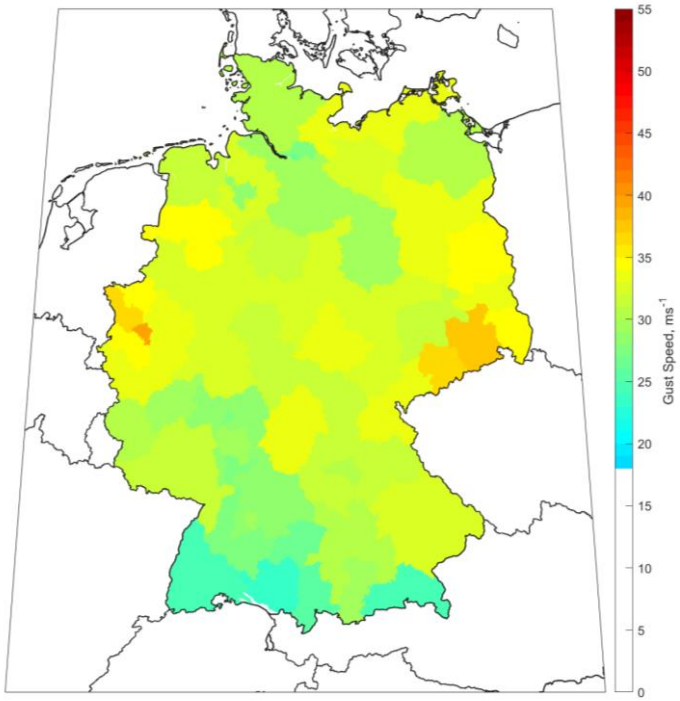

Figure 11 - Maximum gust speed covering at least 10% of each CRESTA in Germany.

4.3 Storm Clustering

When considering the economic and social impacts of storms, the concept of clustering - whereby windstorms occur in groups - is of critical importance. Clustering may be observed over a multi-day timescale whereby multiple storms occur in sequence and are strongly physically linked or over a seasonal or even decadal cycle whereby background conditions favorable for storm generation and strengthening persist, leading to multiple major events within a season (e.g. Dacre and Pinto, 2020). Given the Solvency II laws, the occurrence of multiple storms within a year, typically the time window for an insurance contract, can thus lead to large market impacts, as a part of the aggregated loss may not be covered. There are also concerns over multiple storm systems occurring within an event definition window for loss, which is commonly 72 hours, but varies.

A recent example of storm clustering affecting Northern Europe was the Dudley-Eunice-Franklin cluster in 2022 (e.g., Mühr et al., 2022), while major historical examples include the winters of 1990, 1993, 1999 or 2007, where multiple major storms affected Europe (Pinto et al., 2014).

The Impact Forecasting stochastic event set is taken from GCM output. Clustering is therefore inherently included in the model. This is argued to be a major advantage of using the GCM. The stochastic event set is taken from physically consistent GCM simulations and the storm clusters and grouping within years are extracted as simulated. Storms are never moved between years and clusters of storms are never broken. The building of the event set does then not require any re-clustering of initially independent storms based on statistics derived from the observed history.

5 Vulnerability Component

The vulnerability functions within the model estimate the likely damage to a risk at a given wind speed. The input to the vulnerability function is the gust speed and the output is the loss as a percentage of the TIV, known as the damage ratio (DR). The function is split into two components, the chance of loss (COL) and the conditional mean damage ratio (CMDR) which is the expected damage given that a loss is occurring. For a windstorm, the COL is low across most of the affected areas; if a postcode is hit by a 25 ms^{-1} gust, most of the buildings will not experience any loss.

As an example, we consider a building with a TIV of 100,000 Euros exposed to a gust speed of 35 ms^{-1}. If the COL is 0.2 and the CMDR is 0.3, then the building experiences a loss 20% of the time with an average loss value of 30,000 Euros. The overall average loss for this risk in this event can be calculated deterministically as TIV*COL*CMDR, giving 6,000 Euros.

A sampling approach is used by the model engine. Random number generation is used to determine the hazard value from the distribution within the administrative unit and to determine the loss ratio from the vulnerability distribution. In the example above, given a sufficiently large sample size, the model engine would return an average loss for this risk and this event of 6,000 Euros as calculated above but the individual samples would contain a range of values, 70% should have 0 loss while the others contain values determined by the uncertainty in the vulnerability function.

To describe vulnerability uncertainty, the model uses damage matrixes, wherein the hazard intensity is divided into bins, which are integer values of gust speed, and the estimated DR is divided into bins with each having a probability of being affected, therefore variation in the DR is considered. Figure 12 illustrates this by showing the spread of damage ratio probabilities at three different gust speed bins for an example vulnerability function. The lowest damage bin has a damage ratio of 0, corresponding to no loss. The figure shows how the change of no loss decreases from 96.3% at 30ms^{-1} to 15.5% at 50ms^{-1}.

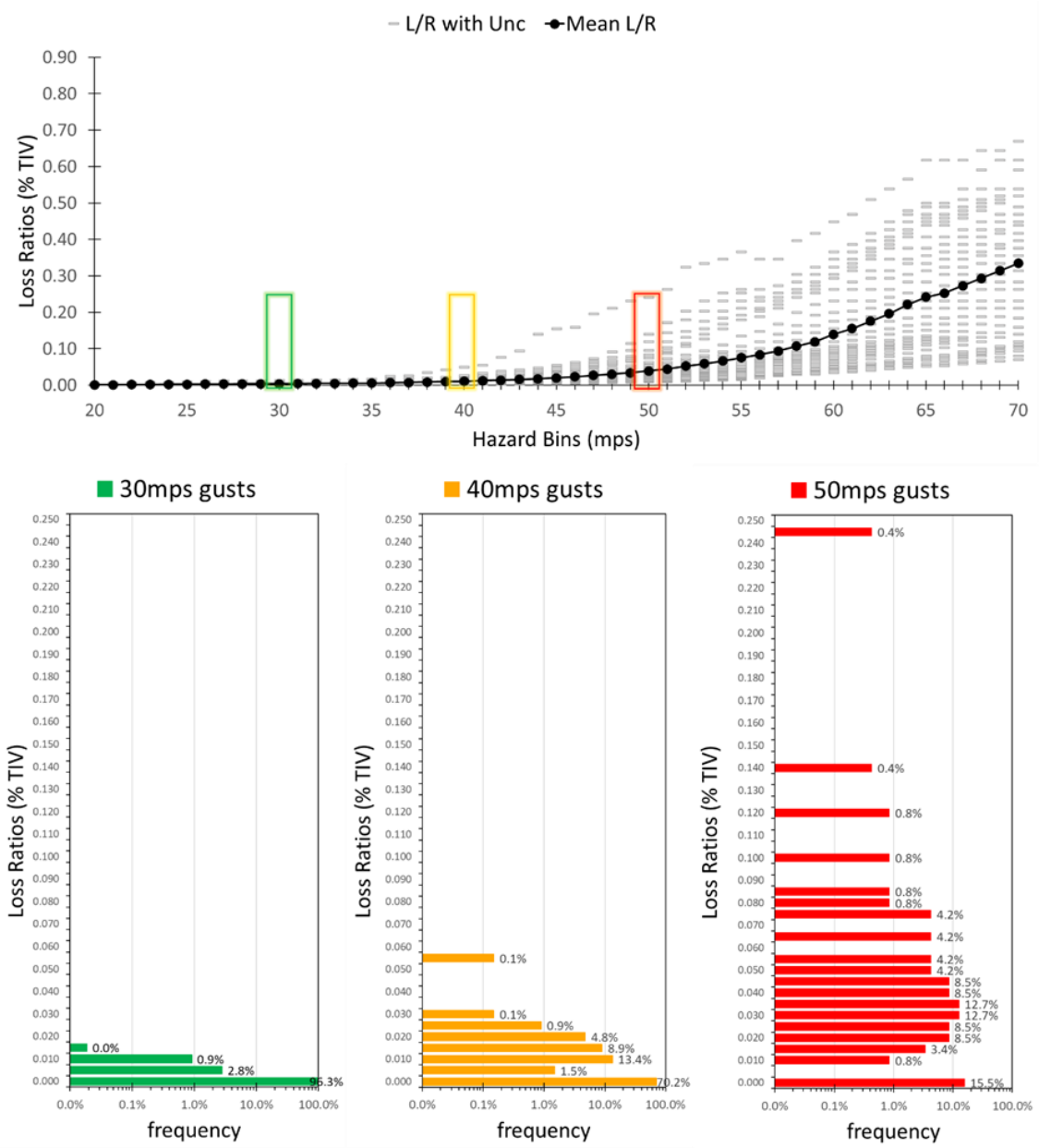

Figure 12 - Example of the uncertainty distribution of the CMDR for different gust values for an example residential damage function.

6 Financial Component

This section covers very briefly how losses are calculated in the model. For more details see the ELEMENTS user guide (https://www.aon.com/reinsurance/getmedia/f182b551-a03b-417c-8c71-8374d1918bd5/models_if_brochure.pdf). The model is primarily designed to run in ELEMENTS, Impact Forecasting's proprietary modelling platform. The model may also be available through third party platforms such as Nasdaq.

After importing a portfolio, a user can run the model through ELEMENTS. There are options to run either the historic or stochastic model. They must specify some desired output conditions including return periods for a stochastic model run. ELEMENTS will by default recommend an appropriate number of damage samples to run, though this can be changed. When running the model, for each damage sample, ELEMENTS takes each risk in the portfolio and determines a hazard value at that risk from the distribution given in the model files for the appropriate administrative unit. Random number generation is used to determine the hazard value in each sample. The model engine then applies the appropriate vulnerability functions and through random number generation selects a damage bin from the distribution. The damage ratio associated with that bin is then applied to the TIV given for that risk and a loss for that risk in that sample is returned. This value is the Ground Up (GU) loss, which is before any application of financial conditions. After applying financial conditions such as deductibles, the Gross loss is returned.

The primary output from ELEMENTS is an Event Loss Table (ELT) which lists the GU and Gross losses per event for the portfolio. This can be the mean loss from all samples or can contain all sample losses individually. It is possible to obtain an ELT for the entire portfolio or at specified break-outs such as per region, per occupancy type, etc.

The Occurrence Exceedance Probability (OEP) curve is then derived from the ELT. For each year, the maximum loss is taken. These are then ordered by the loss value. Each loss was from a modelled year and with an associated frequency and so the frequency of each loss is the cumulative sum of losses in the table. The return period is the reciprocal of frequency and linear interpolation is used to output the losses at requested return periods. The Annual Exceedance Probability (AEP) curve is calculated in the same way except the total loss per year is used rather than the maximum.

7 References

Born K., Ludwig P., and Pinto J. G. (2012) Wind Gust Estimation for Mid-European Winter Storms: Towards a Probabilistic View, Tellus A, 64, 17471, https://doi.org/10.3402/tellusa.v64i0.17471

Dacre H. F., and Pinto J. G. (2020) Serial clustering of extratropical cyclones: a review of where, when and why it occurs, npj Climate and Atmospheric Science, 3, https://doi.org/10.1038/s41612-020-00152-9

Dee et al. (2011) The ERA-Interim reanalysis: configuration and performance of the data assimilation system, Quarterly Journal of the Royal Meteorological Society, 137, 553-597, https://doi.org/10.1002/qj.828

Haas R., and Pinto J. G. (2012) A combined statistical and dynamical approach for downscaling large-scale footprints of European windstorms. Geophysical Research Letters, 39, L23804, https://doi.org/10.1029/2012GL054014

Haas R., Pinto J. G., and Born K. (2014) Can dynamically downscaled windstorm footprints be improved by observations through a probabilistic approach? Journal of Geophysical Research – Atmospheres, 119, 713-725, https://doi.org/10.1002/2013JD020882.

Kalnay et al. (1996) The NCEP-NCAR 40-year reanalysis project, Bulletin of the American Meteorological Society, 77, 437-472, https://doi.org/10.1175/1520-0477(1996)077%3C0437:TNYRP%3E2.0.CO;2

Karremann M. K., Pinto J. G., von Bomhard P. J., and Klawa M. (2014) On the clustering of winter storm loss events over Germany, Natural Hazards and Earth System Sciences, 14, 2041-2052, https://doi.org/10.5194/nhess-14-2041-2014.

Klawa M., and Ulbrich U. (2003) A model for the estimation of storm losses and the identification of severe winter storms in Germany, Natural Hazards and Earth System Science, 3, 725-732, https://doi.org/10.5194/nhess-3-725-2003

Leckebusch G. C., Weimer A., Pinto J. G., Reyers M. and Speth P. (2008) Extreme windstorms over Europe in present and future climate: a cluster analysis approach, Meteorologische Zeitschrift, 17, 67-82, https://doi.org/10.1127/0941-2948/2008/0266.

Mühr B., Eisenstein L., Pinto J. G., Knippertz P., Mohr S., and Kunz M. (2022) CEDIM Forensic Disaster Analysis Group (FDA): Winter storm series: Ylenia, Zeynep, Antonia (int: Dudley, Eunice, Franklin) – February 2022 (NW & Central Europe), https://doi.org/10.5445/IR/1000143470

Pinto, J. G., Karremann M. K., Born K., Della-Marta P. M., and Klawa M. (2012) Loss potentials associated with European windstorms under future climate conditions, Climate Research, 54, 1–20, https://doi.org/10.3354/cr01111.

Pinto J. G., Gómara I., Masato G., Dacre H. F., Woollings T., and Caballero R. (2014) Large-scale dynamics associated with clustering of extra-tropical cyclones affecting Western Europe,

Journal of Geophysical Research – Atmospheres, 119, 13704-13719, https://doi.org/10.1002/2014JD022305

Rockel B., Will A., and Hense A. (2008) Special issue: regional climate modelling with COSMO-CLM (CCLM). Meteorologische Zeitschrift, 17, 347-348, https://doi.org/10.1127/0941-2948/2008/0309

Uppala et al. (2005) The ERA-40 reanalysis, Quarterly Journal of the Royal Meteorological Society, 131, 2961-3012, https://doi.org/10.1256/qj.04.176

S2. Additional Tables and Figures

Table S1: Historical event set of insured winter windstorms in Aon's IF Euro WS model in the period 1990-2020, including storm name and event date (as yyyy-mm-dd).

STORM	DATE
Daria	1990-01-25
Anatol	1999-12-03
Lothar	1999-12-26
Martin	1999-12-27
Jeanett	2002-10-27
Erwin	2005-01-07
Kyrill	2007-01-16
Emma	2008-03-01
Klaus	2009-01-24
Xynthia	2010-02-27
Tappani	2011-12-26
Christian	2013-10-26
Xaver	2013-12-04
Dirk	2013-12-23
Tini	2014-02-12
ElonFelix	2015-01-08
MikeNiklas	2015-03-31
Thomas	2017-02-23
Zeus	2017-03-06
Xavier (2017)	2017-10-06
Herwart	2017-10-29
Eleanor	2018-01-02
Friederike	2018-01-18
Isaias	2019-02-08
Eberhard	2019-03-10
Sabine	2020-02-09

Table S2: List of top 20 storms from ERA5 for 1979-2019 for Core Europe. Information includes the storm name, storm rank, event period and value of Loss Index (LI). Shown are only the common 20 most extreme storms with ERA-Interim.

Rank	Storm name	Start date	End date	LI	Original Rank
1	**Vivian, Wiebke**	1990-02-26	1990-02-28	769794.9	1
2	**Kyrill, Lancelot**	2007-01-18	2007-01-20	724570.7	2
3	**Daria**	1990-01-25	1990-01-28	691602.4	3
4	**Kurt, Lothar, Martin**	1999-12-23	1999-12-26	639103.5	5
5	**13 Jan 84, 14 Jan 84**	1984-01-12	1984-01-15	573311.1	6
6	**Verena**	1993-01-12	1993-01-15	527002.6	7
7	**Jeanett, Katharina, Lara**	2002-10-25	2002-10-28	503317.0	10
8	**Nov 84**	1984-11-22	1984-11-24	487979.3	11
9	**Braer, 13 Jan 93**	1993-01-11	1993-01-14	485094.7	12
10	**Andrea, Ulli**	2012-01-03	2012-01-05	482571.3	13
11	**Lore**	1994-01-25	1994-01-28	468993.4	15
12	**CE1**	1997-02-24	1997-02-26	435918.6	16
13	**Herta**	1990-02-01	1990-02-04	435159.4	18
14	**Dec-93**	1993-12-08	1993-12-11	423932.7	19
15	**Mike, Niklas**	2015-03-29	2015-03-31	423640.9	20
16	**Franz, Hanno, Gerhard**	2007-01-10	2007-01-13	421784.4	21
17	**Jan-95**	1995-01-21	1995-01-24	416758.5	22
18	**Johanna, Kirsten**	2008-03-10	2008-03-12	396952.7	23
19	**Gernot, Ingmar, Burglind**	2018-01-01	2018-01-03	391770.7	24
20	**11 Feb 90**	1990-02-11	1990-02-14	390314.1	25

Table S3: Same as Table S2, but for ERA-Interim.

Rank	Storm name	Start date	End date	LI	Original Rank
1	**Vivian, Wiebke**	1990-02-26	1990-03-01	81503.9	1
2	**Daria**	1990-01-25	1990-01-28	76591.4	2
3	**Kyrill, Lancelot**	2007-01-18	2007-01-20	70723.7	3
4	**Kurt, Lothar, Martin**	1999-12-25	1999-12-27	67481.7	4
5	**Jeanett, Katharina, Lara**	2002-10-25	2002-10-28	64321.1	5
6	**13 Jan 84, 14 Jan 84**	1984-01-12	1984-01-15	56511.3	6
7	**Nov 84**	1984-11-22	1984-11-25	51238.6	7
8	**Dec-93**	1993-12-08	1993-12-11	50957.0	8
9	**Mike, Niklas**	2015-03-29	2015-03-31	49616.4	9
10	**Verena**	1993-01-12	1993-01-15	49027.0	11
11	**Andrea, Ulli**	2012-01-03	2012-01-06	48946.2	12
12	**Johanna, Kirsten**	2008-03-10	2008-03-13	47165.6	14
13	**CE1**	1997-02-24	1997-02-26	47125.3	15
14	**Lore**	1994-01-25	1994-01-28	46779.8	16
15	**Jan-95**	1995-01-21	1995-01-24	46234.1	18
16	**Gernot, Ingmar, Horst, Burglind**	2018-01-01	2018-01-04	45150.2	19
17	**13 Jan 93**	1993-01-11	1993-01-14	44229.0	20
18	**Herta**	1990-02-01	1990-02-04	43373.9	24
19	**11 Feb 90**	1990-02-11	1990-02-14	41585.6	27
20	**Franz, Hanno, Gerhard**	2007-01-10	2007-01-13	38258.8	33

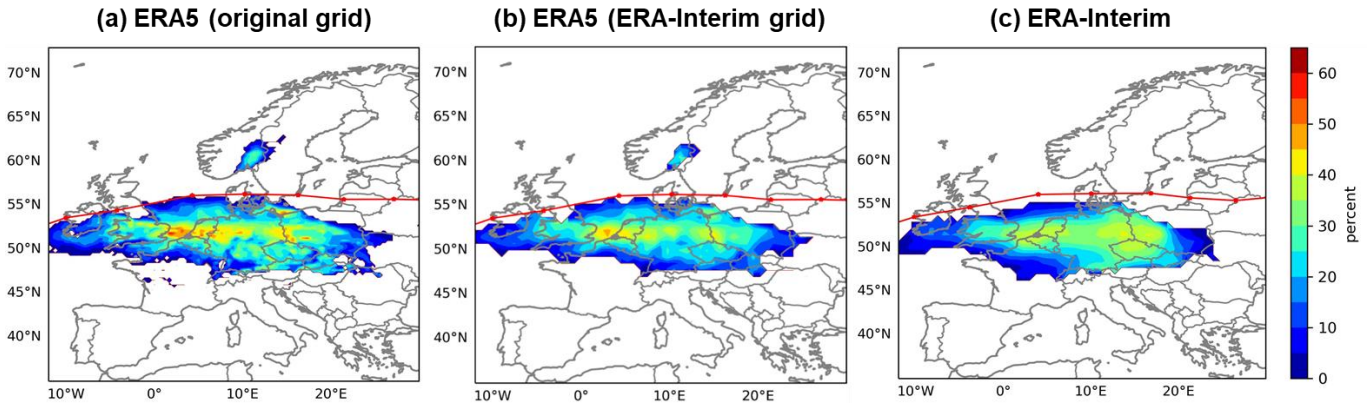

Figure S1: Wind gust footprint for storm Irina in October 2002 based on ERA5 (a), ERA5 re-gridded to the ERA-Interim grid (b), and ERA-Interim (c). Shown is the largest exceedance (in percent) of the 98th percentile of daily maximum wind gust within 72 hours. The red line and dots denote the cyclone track derived from ERA5 (a, b) and ERA-Interim (c) using the tracking algorithm of *Pinto et al. (2005)*.

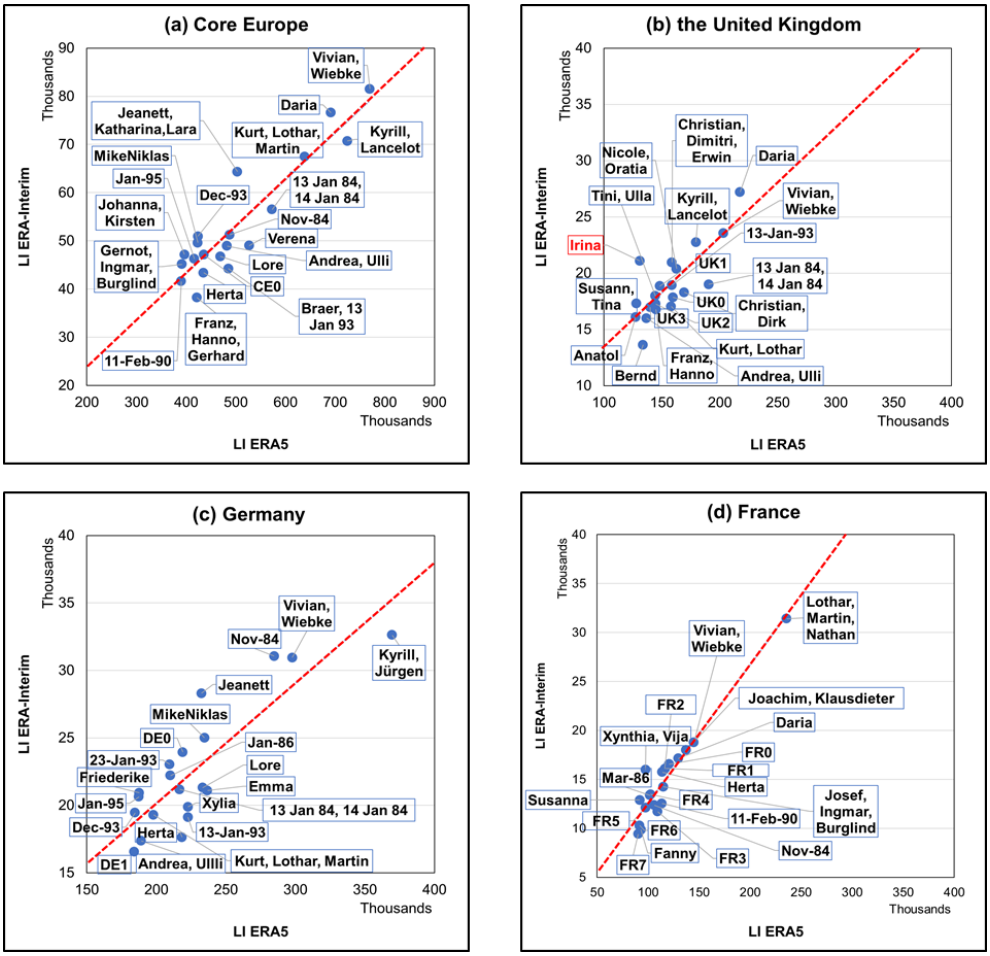

Figure S2: Comparison of loss values (in thousands) based on LI ERA5 (x-axis) and LI ERA-Interim (y-axis). Depicted are the common 20 most extreme storms in the period 1979-2019 for (a) Core Europe, (b) the United Kingdom, (c) Germany, and (d) France. Corresponding storm names to each data point are marked with a blue line. Storms without a formal name are named based on the region (e.g. CE for Core Europe) and the loss value (starting for zero for storm with highest loss). The red dashed line denotes the linear regression line. Outlier storms based on the IQR method (see section 4.2) are marked in red. Please note the different scales.

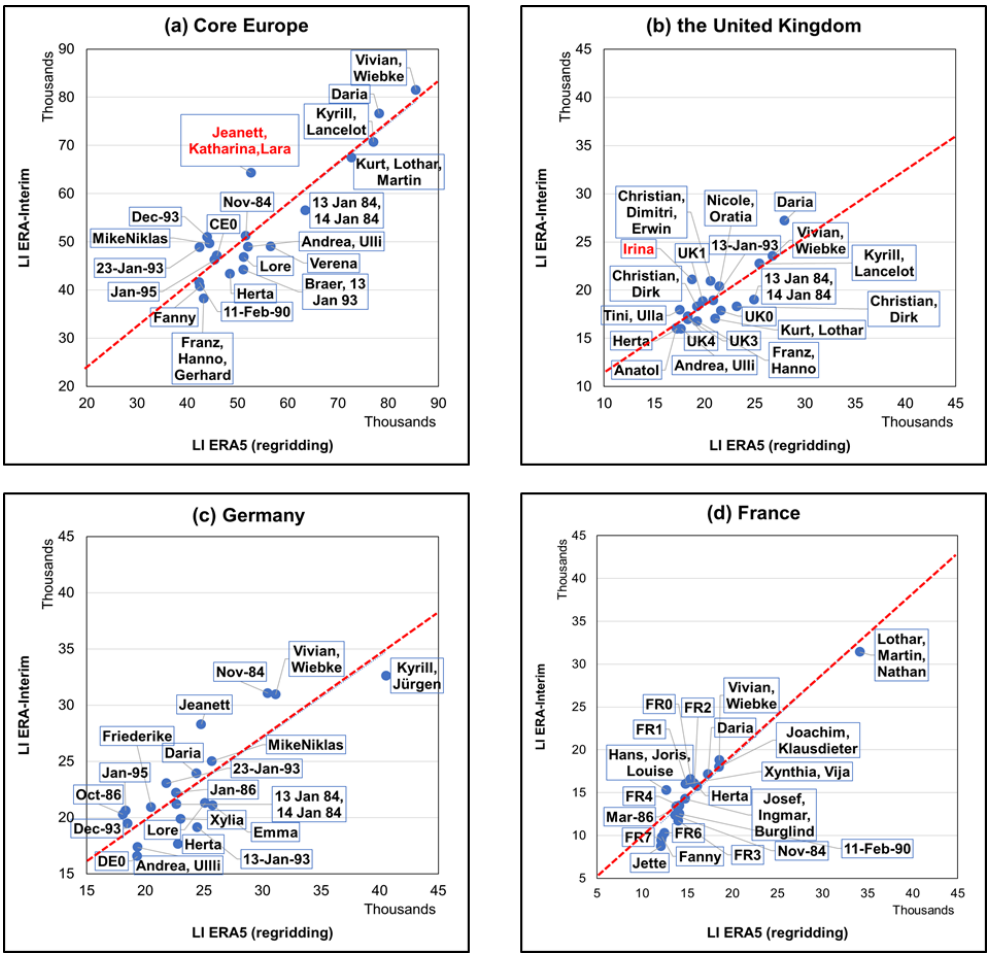

Figure S3: Comparison of loss values (in thousands) based on LI ERA5 (x-axis) and LI ERA-Interim (y-axis). Depicted are the common 20 most extreme storms in the period 1979-2019 for (a) Core Europe, (b) the United Kingdom, (c) Germany, and (d) France. Corresponding storm names to each data point are marked with a blue line. Storms without a formal name are named based on the region (e.g. CE for Core Europe) and the loss value (starting for zero for storm with highest loss). The red dashed line denotes the linear regression line. Outlier storms based on the IQR method (see section 4.2) are marked in red. Please note that LI ERA5 is calculated from ERA5 gust data re-gridded to the ERA-Interim grid.

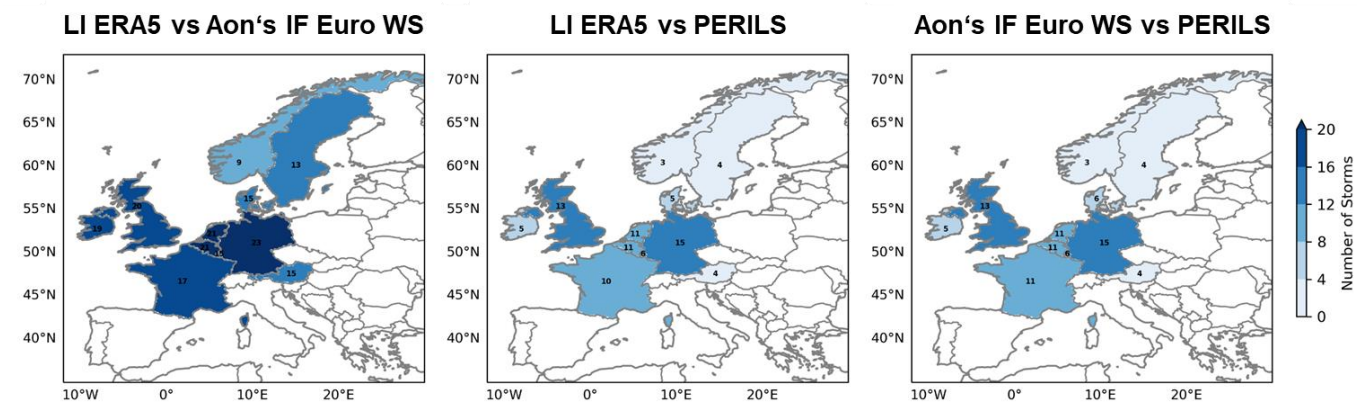

Figure S4: Number of common storms per country for LI ERA5 vs Aon's IF Euro WS model (left), LI ERA5 vs PERILS (middle), and Aon's IF Euro WS model vs PERILS (right).

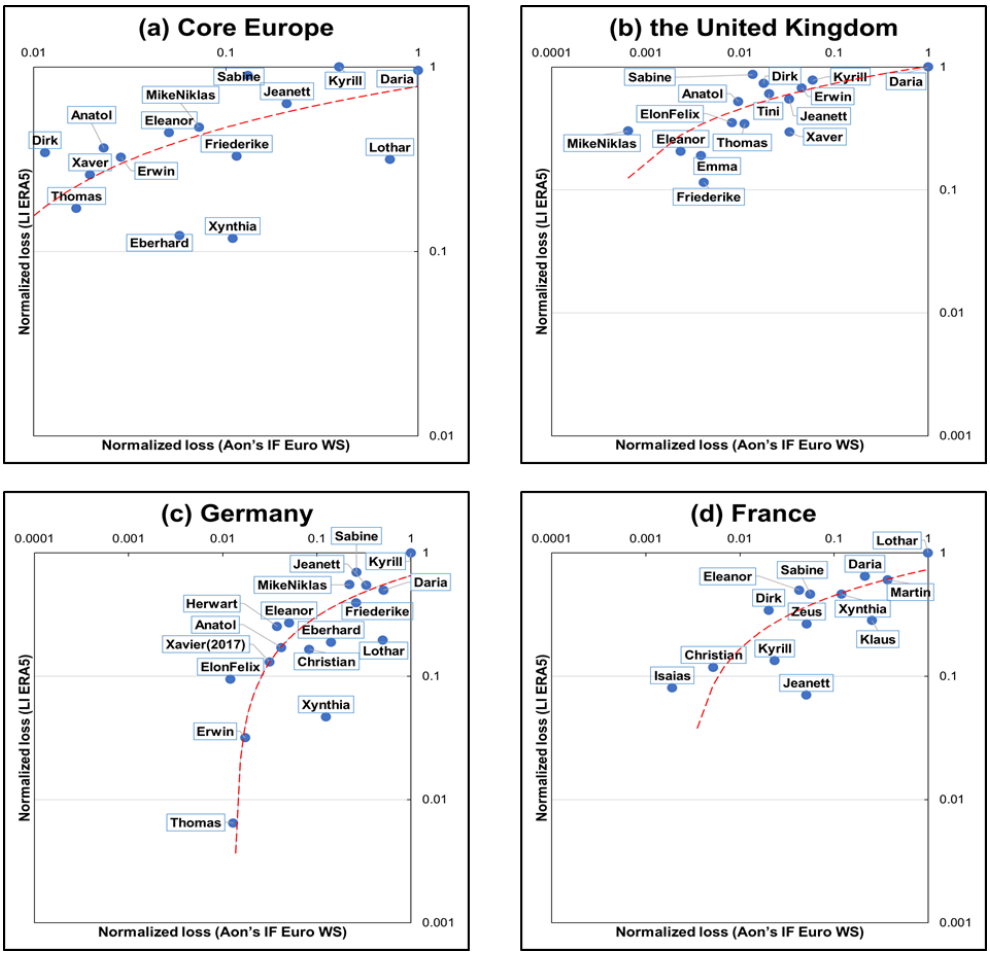

Figure S5: Comparison of normalized loss values between Aon's IF Euro WS model (x-axis) and LI ERA5 (y-axis). Depicted are the common most extreme storms for the period 1990-2020 for (a) Core Europe, (b) the United Kingdom, (c) Germany, and (d) France. A logarithmic scale is used for the axes. The red dashed line denotes the logarithmic regression. Outlier storms based on the IQR method (see section 4.2) are marked in red. LI ERA5 is calculated for 24-hour windows. Please note the different scales.

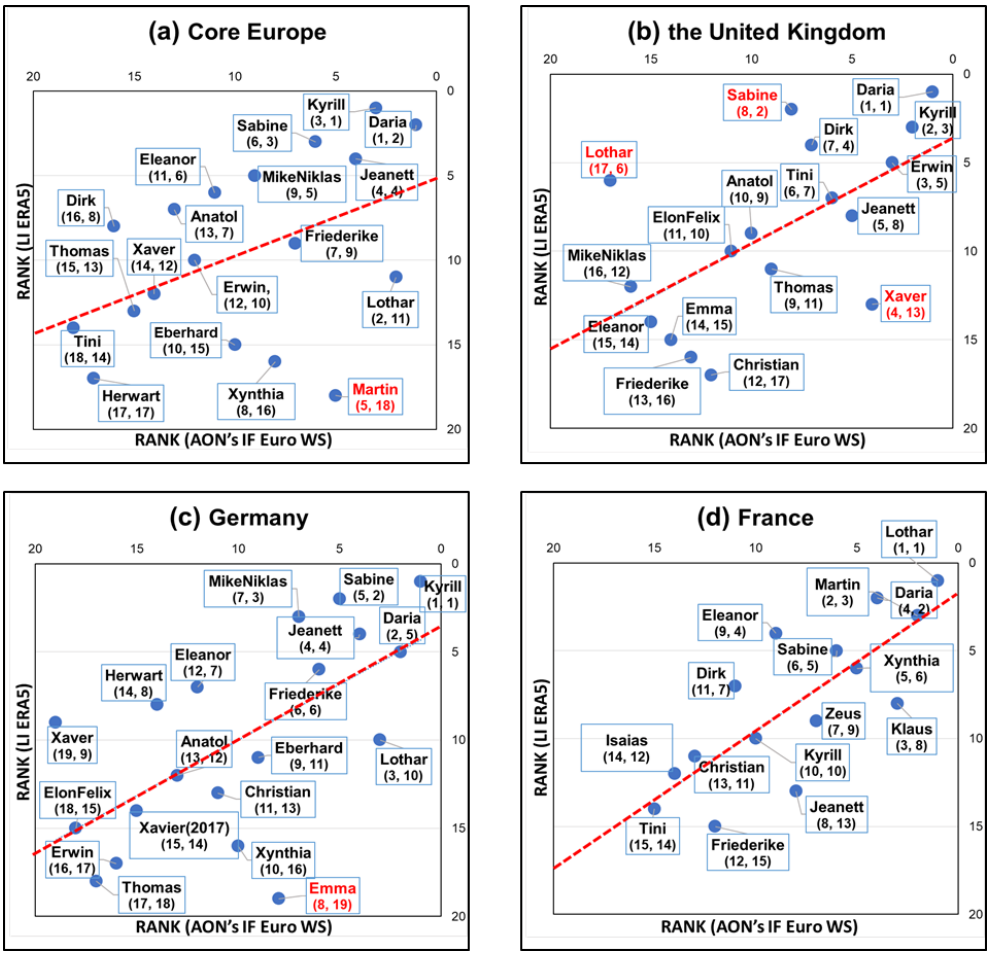

Figure S6: Same as Figure S5, but for the comparison of storm ranks. The values in brackets indicate the rank (first value Aon's model, second value ERA5).